NPS-59Mx74051

NAVAL POSTGRADUATE SCHOOL

Monterey, California

THE THERMAL PERFORMANCE OF AIR-COOLED CIRCUIT BOARDS USED IN STANDARD ELECTRONIC PACKAGE DESIGNS

by

Paul J. Marto

Matthew D. Kelleher

20 May 1974

Prepared for:
val Electronics Laboratory Center
n Diego, California 92152

NAVAL POSTGRADUATE SCHOOL
Monterey, California

Rear Admiral Mason Freeman
Superintendent

Jack R. Borsting
Provost

The work reported herein was supported by the Naval Electronics Laboratory Center, Code 4400, San Diego, California 92152.

This report was prepared by:

UNCLASSIFIED

SECURITY CLASSIFICATION OF THIS PAGE *(When Data Entered)*

REPORT DOCUMENTATION PAGE		READ INSTRUCTIONS BEFORE COMPLETING FORM
1. REPORT NUMBER NPS-59Mx74051	2. GOVT ACCESSION NO.	3. RECIPIENT'S CATALOG NUMBER
4. TITLE *(and Subtitle)*		5. TYPE OF REPORT & PERIOD COVERED Final Report
		6. PERFORMING ORG. REPORT NUMBER
7. AUTHOR*(s)* Paul J. Marto Matthew D. Kelleher		8. CONTRACT OR GRANT NUMBER*(s)*
9. PERFORMING ORGANIZATION NAME AND ADDRESS Naval Postgraduate School Monterey, CA 93940, Code 59Mx		10. PROGRAM ELEMENT, PROJECT, TASK AREA & WORK UNIT NUMBERS WR-4-9072
11. CONTROLLING OFFICE NAME AND ADDRESS Naval Electronics Laboratory Center Code 4400, San Diego, CA 92152		12. REPORT DATE 20 May 1974
		13. NUMBER OF PAGES 44
14. MONITORING AGENCY NAME & ADDRESS*(if different from Controlling Office)*		15. SECURITY CLASS. *(of this report)* UNCLASSIFIED
		15a. DECLASSIFICATION/DOWNGRADING SCHEDULE

16. DISTRIBUTION STATEMENT *(of this Report)*

Approved for public release, distribution unlimited.

17. DISTRIBUTION STATEMENT *(of the abstract entered in Block 20, if different from Report)*

18. SUPPLEMENTARY NOTES

19. KEY WORDS *(Continue on reverse side if necessary and identify by block number)*

Electronics cooling, liquid crystals, convection heat transfer.

20. ABSTRACT *(Continue on reverse side if necessary and identify by block number)*

A test section was designed and constructed to model air-cooled printed circuit boards containing integrated circuit components as proposed for Naval standard package designs.

Thermal performance data are presented for air flow rates to 3.38 CFM across fiberglass/epoxy and aluminum core circuit boards, each containing nine resistor elements to simulate IC components. Hot spot areas on the boards are shown using both liquid crystals and thermocouple data.

DD FORM 1 JAN 73 1473 EDITION OF 1 NOV 65 IS OBSOLETE
S/N 0102-014-6601 |

UNCLASSIFIED

SECURITY CLASSIFICATION OF THIS PAGE *(When Data Entered)*

20. Continued

Results show that in designing such standard packages, care must be taken to avoid obstructions in the air flow path. These obstructions can cause poorly circulating flow regions near the circuit boards, leading to hot spots and poor thermal performance of the IC components. The use of an aluminum core circuit board can significantly reduce this hot spot problem.

Recommendations for continued work are provided.

ACKNOWLEDGEMENT

The authors wish to thank Lieutenants D. V. Colley, J. E. Faltisco, and J. P. McComas, USN, who participated in portions of this work as part of a project laboratory course in Mechanical Engineering. Mr. Thomas F. Christian gave valuable support in fabricating several power supplies and electronic test boards. Their efforts and the advice of our colleagues, Dr. T. E. Cooper and Dr. T. Sarpkaya contributed significantly toward the successful completion of this research.

TABLE OF CONTENTS

1. INTRODUCTION

Recent advances in the design of electronic devices have led to the microminiaturization of electronic circuits, using integrated circuit (IC) components and large scale integration (LSI) devices. Because of the higher power densities in these new circuits, the importance of adequate cooling is readily apparent. Substantial research is therefore underway to study efficient means of removing the waste heat generated in electronic equipment without adding significantly to equipment cost [1,2,3,4].[1]

During the past several years, the Naval Electronics Laboratory Center (NELC) has been studying the reliability of Naval electronic equipment. One conclusion of this study is that sophisticated equipment will operate more reliably if packaging and installing standards are established for shipboard environments [5,6]. Proper packaging would allow these microminiaturized electronic devices to operate effectively without overheating.

In this connection, NELC has proposed a Shipboard Electronic Equipment Modular System (SEEMS) using a standardized air transport rack (ATR) case. In particular, their design calls for the use of the long 3/4 ATR case shown in Figure 1. This case will contain a specified number of printed circuit boards each containing an array of IC components as shown in Figure 2. Each circuit board will be mounted within board guides at a centerline spacing of 0.6 inches, or multiples thereof. Two 0.5 inch diameter cylindrical spacers will be used to separate each board guide as shown. Cooling will occur by forced

[1] Numbers in brackets indicate references listed in the Bibliography.

convection of air through the ATR case. Air will enter at the left front of the case, and will flow along an air inlet plenum within the left side of the case. The air will then be directed between each board guide, will flow around the cylindrical spacers, and across each circuit board before exiting out through a plenum on the right.

This packaging design, while it facilitates installation and allows replacement of individual circuit boards with little difficulty, creates a complicated convective flow pattern of air across each board, which cannot be readily analyzed for heat transfer results. Consequently, reliable thermal performance information of the circuit boards must be obtained through a systematic experimental program.

1.1 OBJECTIVE

The objective of this research project is therefore to experimentally model the air flow through the ATR case, to visually observe the flow around the circuit boards, to locate hot spots on each board using both liquid crystals and thermocouples, and to provide thermal performance data of fiberglass/epoxy and aluminum core circuit boards under proposed standard packaging techniques.

2. EXPERIMENTAL APPROACH

2.1 DESCRIPTION OF THE APPARATUS

The apparatus is shown schematically in Figure 3. Air enters the test section through one of two inlets--either a streamlined nozzle (Nozzle Inlet) aligned with the circuit boards, or a small slot (Slot Inlet) aligned perpendicular to the boards. This slot simulates the actual air flow into the ATR case as seen in Figure 1. After passing through the test section, the air flows through a calibrated rotameter and exhausts to the atmosphere through a variable speed blower. Figure 4 is a photograph of the entire experimental apparatus.

The test section was designed to simulate the crossflow within the actual 3/4 ATR case. It is constructed of 1/4 inch thick clear Lexan plastic to allow for flow visualization and liquid crystal thermography at elevated temperatures. It has overall dimensions of 12 inches long, 5 inches high, and 3 inches deep. This depth accommodates three parallel circuit boards equispaced at 0.6 inch on center to conform to the modular board cage design shown in Figure 2. It was assumed that in the ATR case, the air flow would be divided equally into parallel flow channels between each board. Three parallel flow channels were therefore considered sufficient to model actual conditions. The central board is used for data taking while the two outer boards are used for guard heating to better simulate actual ATR operation. Board guides, spacers, electrical connectors, and test section cover details are identical to those proposed for use in the ATR case. Figure 5 is a photograph of the test section.

The circuit boards used are made either of fiberglass/epoxy (.045 inches thick) or aluminum (.062 inches thick) with overall dimensions shown in Figure 6. Nine 16 pin dual-in-line ceramic cased resistors are mounted in an array on the circuit boards to simulate the IC components on actual boards. These resistors are wired together to give equal heat dissipation in each, with an overall board resistance of 18.8 ohms. All leads are wired to the pin connectors located at the bottom of each board. Note in Figure 6 the location of the two cylindrical spacers in relation to the resistors on the circuit boards. These spacers obstruct the air flow and strongly influence the thermal performance of the resistors as shown later in the report.

2.2 INSTRUMENTATION

The pressure drop of the air across the boards was measured with a micromanometer using a system of four static pressure taps at both the inlet and outlet of the test section. In every case in which the pressure drop was measured, it was found to be less than 0.01 inches of water.

The inlet temperature of the air was measured with a standard mercury-in-glass thermometer. The outlet air bulk temperature was measured using five 28 gage, glass insulated, copper-constantan thermocouples wired in parallel. Teflon coated, 36 gage, copper-constantan thermocouples were bonded with epoxy to the top and bottom of each resistor mounted on the central test board. Four additional thermocouples were mounted in a similar fashion to selected resistors on each of the two guard heater boards to monitor their temperatures as well. All these thermocouples were wired to the pin connectors at

the bottom of the circuit boards, and were recorded on a Hewlett Packard 2010C Data Acquisition System. The thermocouples were calibrated against a platinum resistance thermometer using a constant temperature silicon oil bath maintained from 13°C to 147°C. Calibration data showed that all thermocouples were accurate to within ± 1°C.

Power was supplied to the circuit board resistors by means of a three-channel regulated D.C. power supply. Voltage to the test board was recorded using a Cimron digital voltmeter. The current was determined by measuring the voltage drop, using a millivolt potentiometer, across a 0.333 m Ω standard resistor in series with the test board.

Power to the blower was supplied by a regulated AC power supply through a 2.0 KVA variac.

2.3 FLOW VISUALIZATION TECHNIQUE

As mentioned earlier, it was expected that the irregular nature of the geometry of the flow passages would cause disturbances in the flow. The flow entrance is not smooth. With the slot inlet, the flow must first make an abrupt turn and then an abrupt expansion past the board guides before entering the passage between the circuit boards. The presence of the resistors on the boards themselves act as roughness elements to further disturb the flow. The presence of the cylindrical spacers between board guides might also severely disturb the flow. All of this makes it difficult to categorize the nature of the flow and precludes any form of simplified analysis. With these factors in mind it was felt that flow visualization would provide valuable insight into the qualitative nature of the flow. This in turn would help to interpret the quantitative heat transfer data obtained.

The flow visualization system employed in this study was a liquid aerosol generator developed at the Naval Research Laboratory [7,8]. The system consists of two containers, usually one liter laboratory jars. The first container is half filled with liquid DOP [di (2-ethyl-hexyl) - phthalate]. Regulated and filtered compressed air bubbles through the liquid. This creates an aerosol mist of DOP. This aerosol then flows from the first container through a tube to a jet impactor in the second container. The impactor serves to remove the larger aerosol particles (above 1 μ). The aerosol mist then flows into the test section. The light scattering properties of the aerosol are such that it serves as an excellent flow marker to facilitate flow visualization. As with any flow visualization system, however, care must be taken to insure proper illumination of the marker while reducing extraneous reflections.

Two separate injector arrangements were used to introduce the aerosol into the test section. The first consists of a rake of 12 tubes of 0.080 inch inside diameter. The rake has a total span of approximately 2 inches and can be moved to cover different portions of the test section. The major advantage of the rake arrangement is that it allows the flow in a large region of the test section to be observed at one time.

The second method for introducing the aerosol into the test section is simply a single tube of 0.16 inch inside diameter. The advantage of the single tube is that it can be placed at any desired location at the inlet so that localized disturbances can be isolated and observed.

In viewing and photographing the flow patterns using the aerosol or any other flow marker, proper lighting is extremely important and

usually somewhat difficult to achieve. It is necessary that a well collimated slit of light be provided so that only the flow marker in a particular plane is illuminated. Care must be taken to avoid illuminating other parts of the test section which could introduce extraneous reflections. The slit of light must be well collimated to insure that only a narrow sheet of the flow is illuminated. The photographic exposure must be of short enough duration to capture the fluid motion without blurring the exposure. This requires that high intensity light must be used as well as ultrafast film. The camera lens must also be stopped down to the widest aperature which will allow acceptable depth of field.

During this study, the lighting system which was available was only a crudely collimated beam of limited intensity. This proved adequate for visual observation of the flow patterns, however, and yielded photographs of adequate quality.

2.4 LIQUID CRYSTAL THERMOGRAPHY

In order to examine the effect of the complicated air flow on the convective heat transfer process, liquid crystal thermography was employed. This technique gives a vivid visual representation of hot spot locations. The great potential of this technique as a diagnostic and measurement tool has only recently been explored [9].

Liquid crystals [10] are unique materials which have the mechanical properties of a liquid but because of their molecular structure exhibit many of the optical properties of crystals. The property which is of most interest is the color change which the liquid crystals cause as their temperature changes. As the temperature of the liquid crystals is changed, there is a shift in the predominant wavelength of light which is

reflected. At a certain temperature, called the event temperature, this wavelength enters the visible range. Further changes in temperature can be observed as changes in color of the liquid crystals. With increasing temperature, the crystals first appear red, then yellow, then green, then blue, and finally violet before becoming colorless again. The temperature range over which this color change takes place is of the order of 3°C. Because the liquid crystals are normally colorless, it is usual practice to blacken the surface on which they are to be used. This greatly enhances the brilliance of the colors.

The liquid crystals were used to investigate the effect of the flow in the test section on the wall temperature of both a uniformly heated smooth board and a uniformly heated board with nine passive resistors attached. The uniformly heated board shows hot spots caused by the convective air flow only and minimizes temperature variations which are caused by nonuniform distribution of heat sources. A special board was therefore constructed by attaching a piece of Temsheet to a smooth fiber glass/epoxy board. Temsheet is a form of stiff porous paper which has been impregnated with carbon. The carbon impregnation imparts a uniform electrical resistivity to the paper. By attaching electrodes to opposite edges of the Temsheet and passing a current through it, uniform Joulean heating can be generated. The section of Temsheet used in these experiments had a total resistance between electrodes of 18 ohms.

The temsheet circuit board was coated with liquid crystals which changed color in the temperature range of from 59°C to 62°C. Since the Temsheet is a black material, it served as an ideal substrate for the liquid crystals. The coated Temsheet board was placed in the middle of the three sets of board guides. Dummy boards were placed in the other

two sets of guides so that the influence of adjacent boards could be simulated. The dummy board which was placed in the front card guides was made from a thin sheet of clear Plexiglas to allow viewing of the liquid crystal board. For a subsequent set of experiments nine of the ceramic cased resistors mentioned earlier were glued directly to the Temsheet board. These resistors were used only as flow obstructions. With this arrangement it was possible to observe any influence that the resistors and the flow around them had on the surface temperature of the heated Temsheet board.

3. RESULTS AND DISCUSSION

3.1 FLOW VISUALIZATION RESULTS

The flow visualization experiments were carried out over a range of flow rates from 0.7 CFM to 3.35 CFM. These are the flow rates through the space between adjacent boards and as such may be considered to be flow rate per board. If the hydraulic diameter for the space between adjacent boards is used as the significant length, the Reynolds numbers associated with these flow rates encompass a range of from 1035 to 4820. Both the nozzle inlet and the slot inlet were used as well as both aerosol injectors. During these experiments the test circuit board with nine resistors was unheated and was placed in the board guides nearest the front of the test section to make viewing easier.

It was observed that at all Reynolds numbers the flow was not uniform over the board. The flow appeared to be divided into distinct regions. Across the center region of the board the flow appeared as a well-ordered, laminar streaming type of motion. As might be expected there was a narrow wake region downstream of each of the resistors in this area of the board. On the other hand the flow across the upper portion of the board was completely different in character. In this region the flow was recirculating, i.e. the flow was in the form of large vortices which appeared to be trapped in this region. This is understandable based on the geometry of the test section. The flow in this section of the board was obviously being dominated by the cylindrical spacer used between board guides. The nature of the flow over the upper portion of the board at a Reynolds number of 900 is illustrated in Figure 7.

If a Reynolds number based on this cylinder diameter (0.5 inch) is calculated, it is found that this Reynolds number varies from 524 to 2439 for the range of flow rates considered. In this Reynolds number range the flow behind a cylinder is in the form of vortices which are alternately shed from the top and bottom of the cylinder [11]. Of course, the vortex shedding from the cylindrical spacer is influenced by the presence of the top wall and the I.C. boards. The presence of another cylindrical spacer at the upper part of the exit of the test section tends to act as an obstruction which somewhat prevents the flow in this region from exiting. The influence of these two upper board guide spacers explains the recirculating flow region which exists over the upper portion of the board.

This flow pattern was observed in essentially the same form for all Reynolds numbers and for both inlet configurations.

It should be noted that this region of recirculating flow could be expected to be a region of poor convective heat transfer which would adversely affect the temperature of any I. C. elements located in this region.

3.2 LIQUID CRYSTAL THERMOGRAPHY RESULTS

The experiments using the liquid crystal coated Temsheet board were carried out over the same range of flow rates as the flow visualization experiments. Power to the board was varied from 12 watts to 24 watts. For these experiments the board was mounted either in the front guides or in the center guides with the clear Plexiglas board in the front guides. Both the nozzle inlet and the slot inlet were used.

The results from these tests confirm the conclusions drawn from the flow visualization experiments--the region behind the upper cylindrical

spacer is a region of poor convective heat transfer. This is true regardless of where the board is mounted and regardless of which inlet is used. This can be seen quite clearly in Figures 8(a) and 8(b). Both figures are for the flow entering from the slot inlet, with the board mounted in the front guides. Figure 8(a) is for a flow rate of 3.37 CFM with 21.6 watts being dissipated in the board. The upper portion of the board (the blue area in the photograph) is at a temperature of approximately 62°C. The remaining portion of the board (black area) is below 59°C. Figure 8(b) is for a flow rate of 2.36 CFM with the board at 12.2 watts. Both the power and the flow rate have been reduced from those in the previous figure. In this case the hot region has been reduced in size. Even though the size of the hot region is smaller, the photograph shows again that it is still on the upper portion of the board between the two cylindrical spacers. It is evident that the region between the two upper cylindrical spacers is the region where hot spots are most likely to occur due to convective effects. This region should therefore be given special attention in placing components on the circuit boards.

3.3 THERMOCOUPLE RESULTS

A series of 26 runs were made using the thermocouples to monitor temperatures. During these runs, the slot inlet was used, and the inlet air was near 23°C. For each run, the air flow rate was fixed, and the power to the central test board was adjusted until the hottest thermocouple indicated either 75°C, 100°C, or 125°C. The power to the outer guard heater boards was adjusted accordingly so that temperatures on these boards were approximately the same as the temperatures indicated

on the central test board. The first 14 runs were taken using a fiberglass/epoxy test board, while the last 12 runs were taken using an aluminum core test board. For each run, the system was allowed to operate for at least one-half hour after the test variables were changed in order to insure that steady state conditions prevailed.

Temperature Distributions. Figures 9 and 10 show typical resistor temperatures for both the fiberglass/epoxy board and the aluminum core board. The power to the board in each case was approximately 13 watts and the air flow was 0.75 CFM per channel. The number above each resistor designates the temperature measured by the thermocouple epoxied to the top of the resistor. The number below each resistor designates the equivalent temperature on the bottom of the resistor. Note that the central resistor on the glass board has only a single temperature recorded due to a failure in the bottom thermocouple wire during installation. The discrepancy in the air outlet temperature in these two runs, even though the power and flow rate was the same, is misleading. It is due to the fact that this temperature reflects the heating of the air not only from the central test board, but also from the outer guard heater boards. Since the aluminum board was operating at a lower temperature than the glass board, the guard heaters were operating at a correspondingly lower power level in this case. Therefore, the total power from all three boards during Run 15 was less than the total power from all three boards in Run 3.

In Run 3, using the glass board, the temperatures were significantly higher than those in Run 15, using the aluminum board. In Run 3, the hottest resistor was near 125°C whereas with aluminum in Run 15, the hottest resistor was only at 75°C. It is clear therefore that the aluminum board is very effective in reducing the operating temperatures of

the resistors mounted on it. Note also that the location of the hottest resistor is shifted in going from the glass board to the aluminum board.

These results are undoubtedly due to the increased thermal conduction effects using aluminum. The thermal conductivity of the fiberglass/epoxy board is very low, less than 1 BTU/hr ft°F, while that of the aluminum board (6061 - T6 alloy) is near 90 BTU/hr ft°F. It is reasonable to assume then that very little of the resistor heat is conducted away through the glass board, and the heat is dissipated primarily by convection directly from the resistor to the moving air stream. (The effect of radiation is assumed to be small because of the relatively low temperature differences existing within the test section.) Consequently, those resistors near the top of the glass board, which are located within the poorly circulating air region noted earlier, are not cooled effectively and are therefore hotter than those in the moving air stream. On the other hand, with the aluminum board, a sizable fraction of the heat generated by a resistor is conducted through its leads to the aluminum core. The aluminum board then acts as a fin, conducting the heat to nearby heat sinks, and convecting it away to the moving air. This is especially apparent near the two sides of the board where contact is made with the aluminum board guides. The hot spots on the aluminum board therefore appear to be at the top and bottom of the middle row of resistors. The bottom resistor actually is slightly hotter than the top one. The exact reasons for this would require a more complete knowledge of the flow details and therefore warrants further investigation.

This influence of conduction is seen more vividly in Figures 11 through 14, which schematically represent the isotherms near the resistors. For the fiberglass/epoxy board the hottest area is near the

top of the board, where the air is poorly circulating due to the obstruction of the cylindrical spacers. The trend of the isotherms closely follows the liquid crystal results shown in Figure 8, presumably due to a similar convective flow pattern. On the other hand, the isotherms for the aluminum board show that the hottest areas are the top and bottom portions of the middle of the board. Between these areas, a colder region exists due to the moving air stream over the center of the board.

Thermal Performance: The hot spot thermal performance data for both types of boards can be compared using Figures 15 and 16. For a given hot spot temperature of 75, 100, or 125°C, the data show how much power can be dissipated for a given flow rate of air. For example, for a hot spot temperature of 100°C, and an air flow rate of 2 CFM per board, the glass board can dissipate 11.5 watts, whereas the aluminum board can dissipate 24.8 watts. It should be remembered, however, that this data was taken for an air inlet temperature of 23°C. If the ambient air temperature is increased, these hot spot temperatures would increase by approximately the same amount. This is true since the transport properties of air are nearly temperature independent.

The thermal performance data for a given resistor can be put into a more meaningful form for design purposes by representing the data in terms of an average unit thermal conductance, $\bar{h}$ [12]. Therefore, the amount of power which a single resistor, or IC component of the same geometry, can dissipate is given by:

$$P = \bar{h} A_s (\bar{T} - T_\infty) \quad (1)$$

where

P = power dissipated, watts

$\bar{h}$ = average unit thermal conductance, watts/m^2°C

A_s = total surface area of the device, m^2

$\bar{T}$ = average surface temperature of the device, °C

T_∞ = local air temperature, °C

In general, $\bar{h}$ depends upon the conduction, convection, and radiation heat transfer paths from the heat source to the ambient sink. The relative contributions of these modes of heat transfer depend on the test section geometry, the materials' properties, and the local flow conditions and temperature distribution around each resistor. An analysis to determine these contributions is clearly beyond the scope of the present work but would be desirable in the future to help maximize $\bar{h}$ for given design conditions.

During this work, as mentioned earlier, the effect of radiation heat transfer was assumed to be very small. Therefore, heat is assumed to be dissipated from each resistor by convection directly to the moving air and by conduction through the leads to the circuit boards. It is further assumed that since the thermal conductivity of the fiberglass/epoxy board is very small, the influence of conduction upon the experimental results is negligible. Experimental results with the fiberglass/epoxy board should therefore primarily represent convection effects, and should be strongly influenced by flow conditions. An average unit thermal conductance for

convection heat transfer (called the average heat transfer coefficient) was therefore calculated for the fiberglass/epoxy board based upon measured data.

The average heat transfer coefficient was determined as follows. The total power into the test board was divided by nine to give the power dissipated by each resistor. This value was then divided by the total surface area of the resistor (i.e., the top, bottom, and all four sides) and by the average surface temperature difference. The average temperature of each resistor was just the arithmetic average of the top and bottom thermocouple readings. The local air temperature was computed assuming a linear variation between the test section inlet temperature and the bulk outlet temperature. The nine local heat transfer coefficients were then averaged spatially. The six lower resistors in the flow stream were averaged together and the three upper resistors in the poorly circulating region were averaged together. These results are plotted in Figure 17 versus air flow rate across the fiberglass/epoxy board. As expected, the average heat transfer coefficient for those resistors in the air flow stream is much greater than the value for those resistors within the circulating region.

For comparison purposes, the heat transfer coefficient for laminar flow over a flat plate at constant heat flux is plotted as a dashed curve in Figure 17. For this case, Kays [13] gives

$$\frac{\bar{h}\ell}{k} = 0.906\ Pr^{1/3}\ Re_{\ell}^{1/2} \qquad (2)$$

where

ℓ = length of the flat plate, m

Pr = Prandtl number of the fluid

Re_{ℓ} = Reynolds number

Each resistor is treated as a flat plate with a new boundary layer forming at its leading edge. All fluid properties are evaluated at an average film temperature of 50°C.

Notice that the experimental data for the flow stream resistors has the same general dependence on flow rate as the theoretical prediction; namely, a square root dependence as given in Equation (2). However, the experimental data is approximately 25% higher than the theory. Other theoretical results, based upon flow within the entrance region of a rectangular duct, fall substantially lower than those predicted by Equation (2). It appears therefore that the flow may be characterized as laminar, but perhaps due to swirling and large scale mixing effects, the heat transfer is augmented over the theoretical flat plate result [14]. It may also be that the high experimental values for $\bar{h}$ are influenced by conduction and radiation effects which have been neglected. The data for those resistors within the poorly circulating air region is less than the theory predicts and has a weaker dependence upon flow rate. Evidently as the air flow increases, the circulating region experiences a net increase in velocity but not nearly to the same extent as the flow stream experiences. These results serve to point out again that the flow within the test section is complicated and that convective heat transfer results for individual resistors cannot be reliably predicted at this time.

The most convenient thermal parameter for design purposes is the average external thermal resistance, $\bar{R}_{ext}$. If this resistance is known for a device, then the design engineer can predict the device thermal performance for a given ambient condition using the relationship

$$P = \frac{(\bar{T} - T_\infty)}{\bar{R}_{ext}} \qquad (3)$$

Notice that this resistance is the average of all thermal resistances, and includes conduction, convection, and radiation effects. The experimental values of $\bar{R}_{ext}$ for both the fiberglass/epoxy board and the aluminum board are plotted versus air flow in Figure 18. For each board, a resistance is given for the hot region of the board as well as for the cold region. For the glass board, the hot region resistance represents an average of the resistances on the top three resistor elements. The cold region resistance is the average of the lower six resistances. For the aluminum board, the hot region represents the average of the two hot spot resistors seen earlier in Figures 12 and 14, while the cold region represents the average of the remaining seven resistors. It is evident that the aluminum board has a lower thermal resistance due to increased conduction heat transfer. Conduction also reduces the magnitude of temperature variations across the board since the hot and cold region resistances are closer together for aluminum than for the glass board. Notice also the weak dependence of the aluminum board results upon flow rate, indicating again that these results are influenced by conduction heat transfer paths.

4. CONCLUSIONS AND RECOMMENDATIONS

4.1 CONCLUSIONS

Based upon the experimental results obtained, the following conclusions can be made:

1. The presence of the 0.5 inch diameter cylindrical spacers as part of the 3/4 ATR circuit board cage cause a poorly circulating flow region near the top of the board. This poorly circulating flow reduces convective heat transfer and deteriorates the thermal performance of electronic devices mounted in this region.

2. The use of an aluminum core circuit board rather than a fiberglass/epoxy board smooths out temperature variations on the surface of the board and reduces hot spot temperatures significantly.

3. The air flow across each circuit board can be characterized as a complicated laminar flow with large scale mixing. The overall pressure drop across each circuit board is less than 0.01 inches of water.

4. Convective heat transfer results for individual devices mounted upon circuit boards cannot be reliably predicted at this time.

4.2 RECOMMENDATIONS

It is recommended that:

1. The ATR circuit board cage be redesigned to eliminate the cylindrical spacers blocking the air flow.

2. Aluminum circuit boards should be used rather than glass boards whenever this is feasible.

3. The various heat transfer paths from a heat dissipating device to the ambient should be further studied. An appropriate heat transfer model should be developed which includes conduction, convection, and radiation effects so that the overall external thermal resistance can be predicted, and perhaps be minimized for given operating conditions.

4. Since conduction heat transfer can significantly alter the thermal performance of circuit boards, additional research work should be performed to study the advantages of fins and the use of heat pipes to further improve upon performance.

BIBLIOGRAPHY

1. Bergles, A. E., Chu, R. C., and Seely, J. H., "Survey of Heat Transfer Techniques Applied to Electronic Equipment," ASME paper No. 72-WA/HT-39, presented at the ASME Winter Annual Meeting, New York, N. Y., November 26-30, 1972.

2. Boucher, S. G., and Paradis, L. R., "Experimental Heat Transfer Investigations on Modules Mounting Hybrid Packages," 1973 Electronic Components Conference, Washington, D. C., May 14-16, 1973.

3. Aung, W., Bertin, K. I., and Kessler, T. J., "Natural Convection Cooling of Electronic Cabinets Containing Arrays of Vertical Circuit Cards," ASME paper No. 72-WA/HT-40, presented at the ASME Winter Annual Meeting, New York, N. Y., November 26-30, 1972.

4. Baker, E., "Liquid Cooling of Microelectronic Devices by Free and Forced Convection," Microelectronics and Reliability, 11, pp. 213-222, 1972.

5. Hauser, H. K. and Urban, E. C., "Air Transport Equipment Cases and Racking for Multiservice Use," NELC Code 4400, September, 1972.

6. "Electronic Equipment Packaging and Installation Study," Final Report, NELC Code 4400, November 1971.

7. Griffin, O. M. and Votaw, C. W., "The Use of Aerosols for the Visualization of Flow Phenomena," Int. J. Heat Mass Transfer, 16, pp. 217-219, 1973.

8. Griffin, O. M., Ramberg, S. E., Votaw, C. W., and Kelleher, M. D., "The Generation of Liquid Aerosols for the Visualization of Oscillatory Flows," Record of the International Congress on Instrumentation in Aerospace Simulation Facilities, Pasadena, Ca., September 1973.

9. Fergason, J. ., "Liquid Crystals," Scientific American, 211, No. 2, pp. 76-86, August 1964.

10. Cooper, T. E., and Groff, J. P., "Thermal Mapping, via Liquid Crystals of the Temperature Field near a Heated Surgical Probe," J. Heat Transfer, 95, pp. 250-256, May 1973.

11. Schlichting, H., "Boundary Layer Theory," 6th edition, pp. 28-32, McGraw-Hill Book Co., New York, N. Y., 1968.

12. Kreith, F., "Principles of Heat Transfer," 3rd edition, pp. 13-18, Intext Educational Publishers, New York, N. Y., 1973.

13. Kays, W. M., "Convective Heat and Mass Transfer," pp. 221-222, McGraw-Hill Book Co., New York, N. Y., 1966.

14. Bergles, A. E., "Techniques to Augment Heat Transfer," Section 10 of Handbook of Heat Transfer, Rohsenow, W. M., and Hartnett, J. P., editors, McGraw-Hill Book Co., New York, N. Y. 1973.

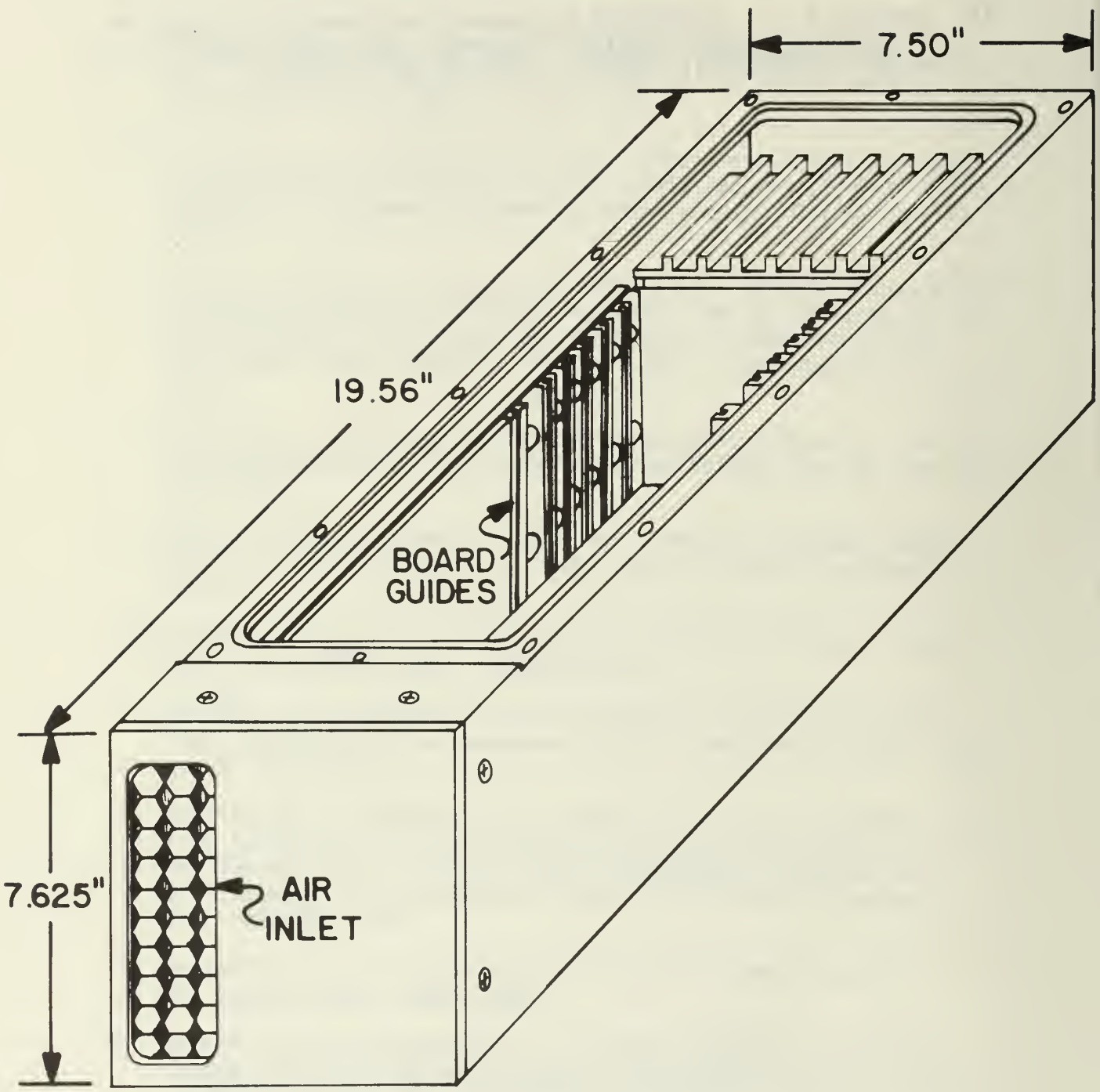

FIGURE 1 PERSPECTIVE VIEW OF LONG 3/4 ATR CASE

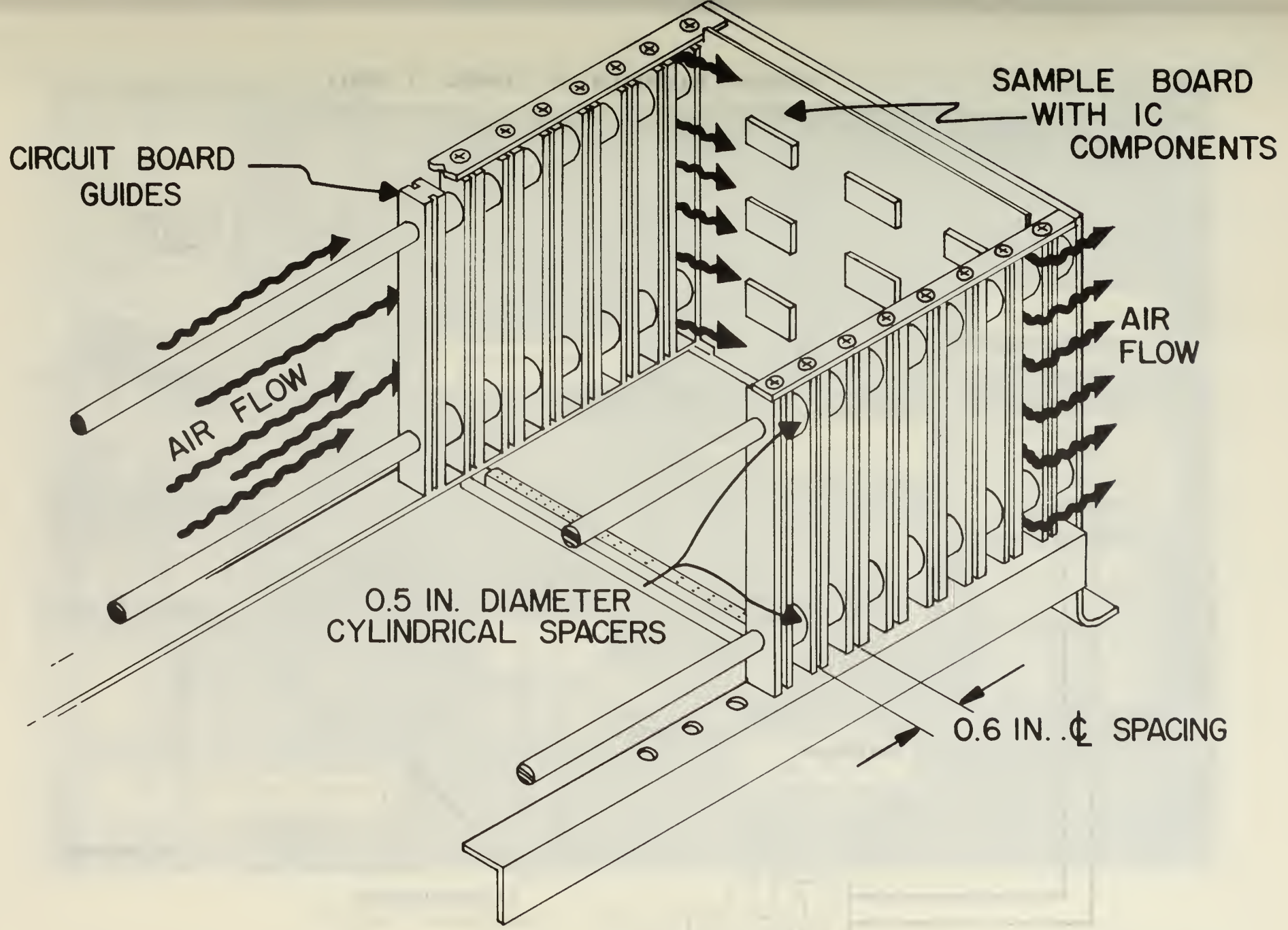

FIGURE 2 PARTIAL ASSEMBLY OF MODULAR CIRCUIT BOARD CAGE

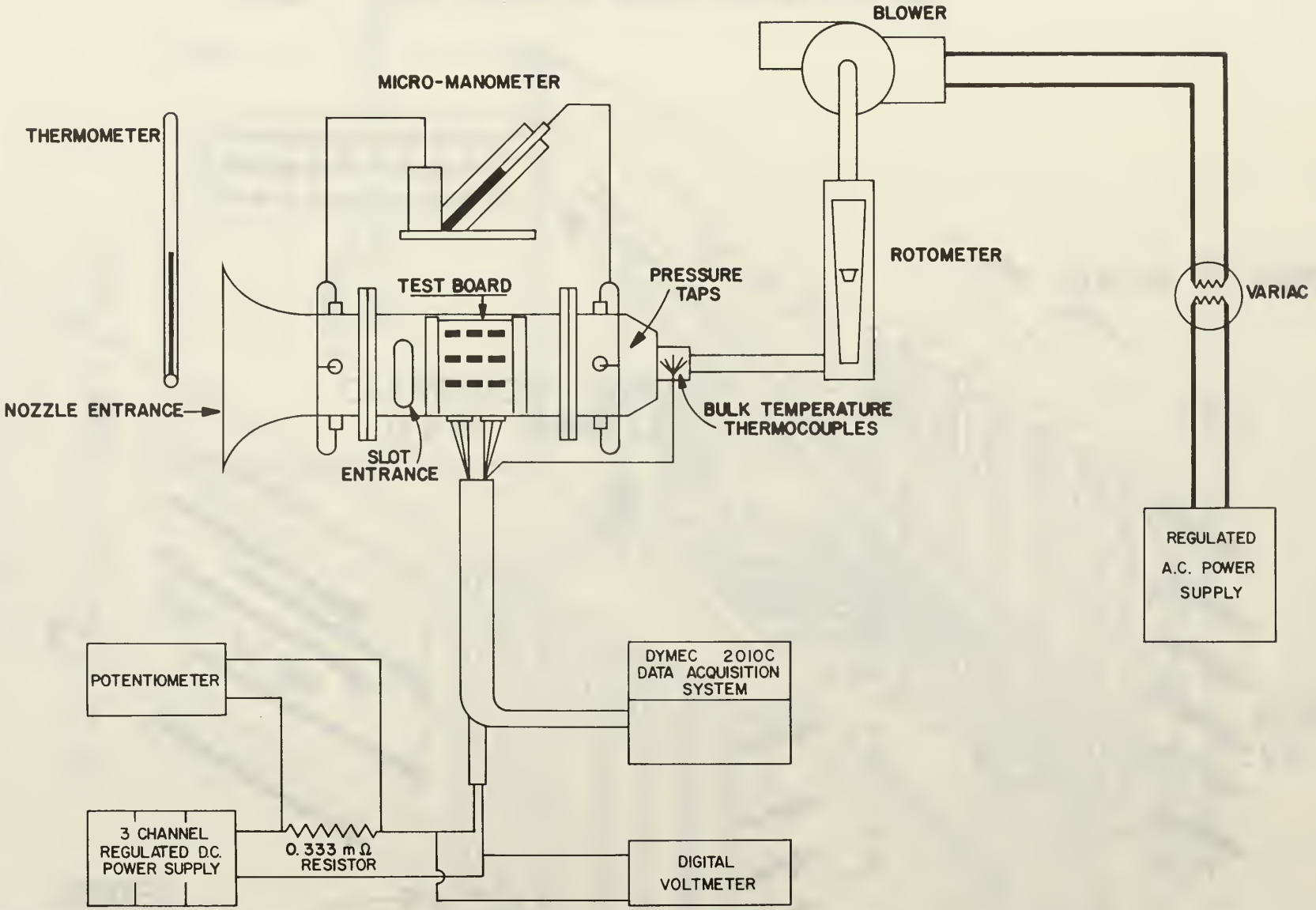

FIGURE 3 SCHEMATIC OF EXPERIMENTAL APPARATUS

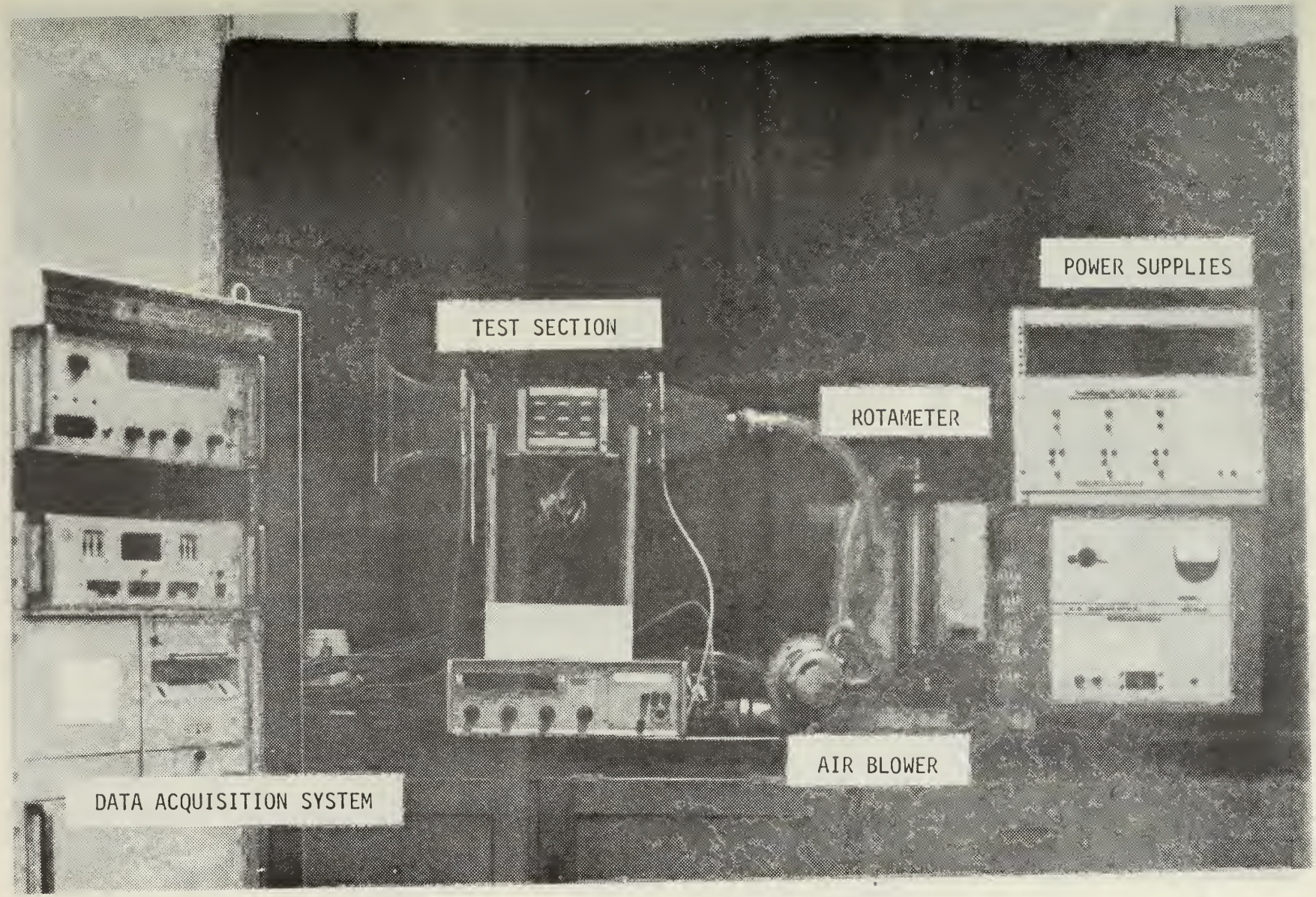

FIGURE 4 PHOTOGRAPH OF EXPERIMENTAL APPARATUS

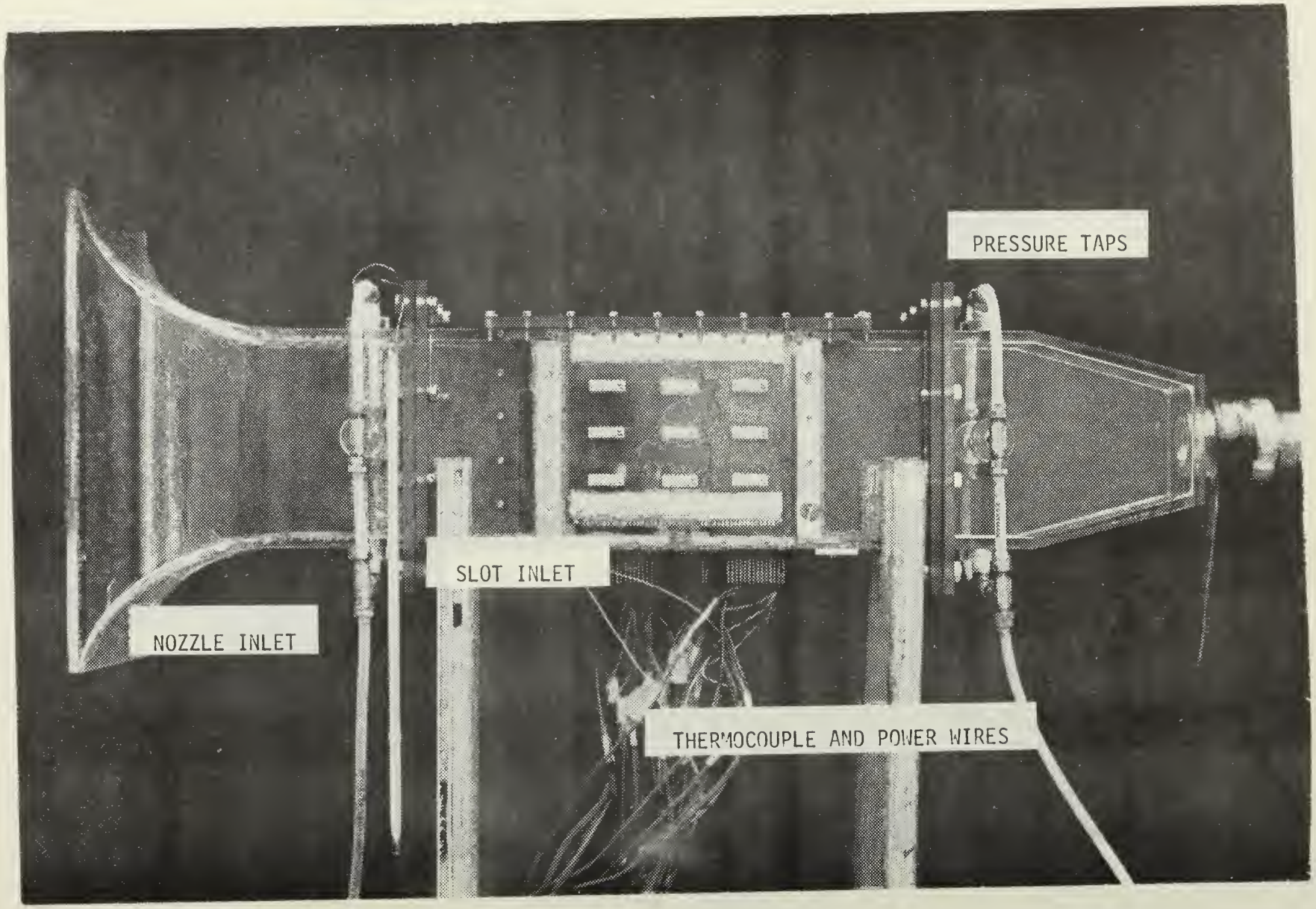

FIGURE 5. PHOTOGRAPH OF TEST SECTION

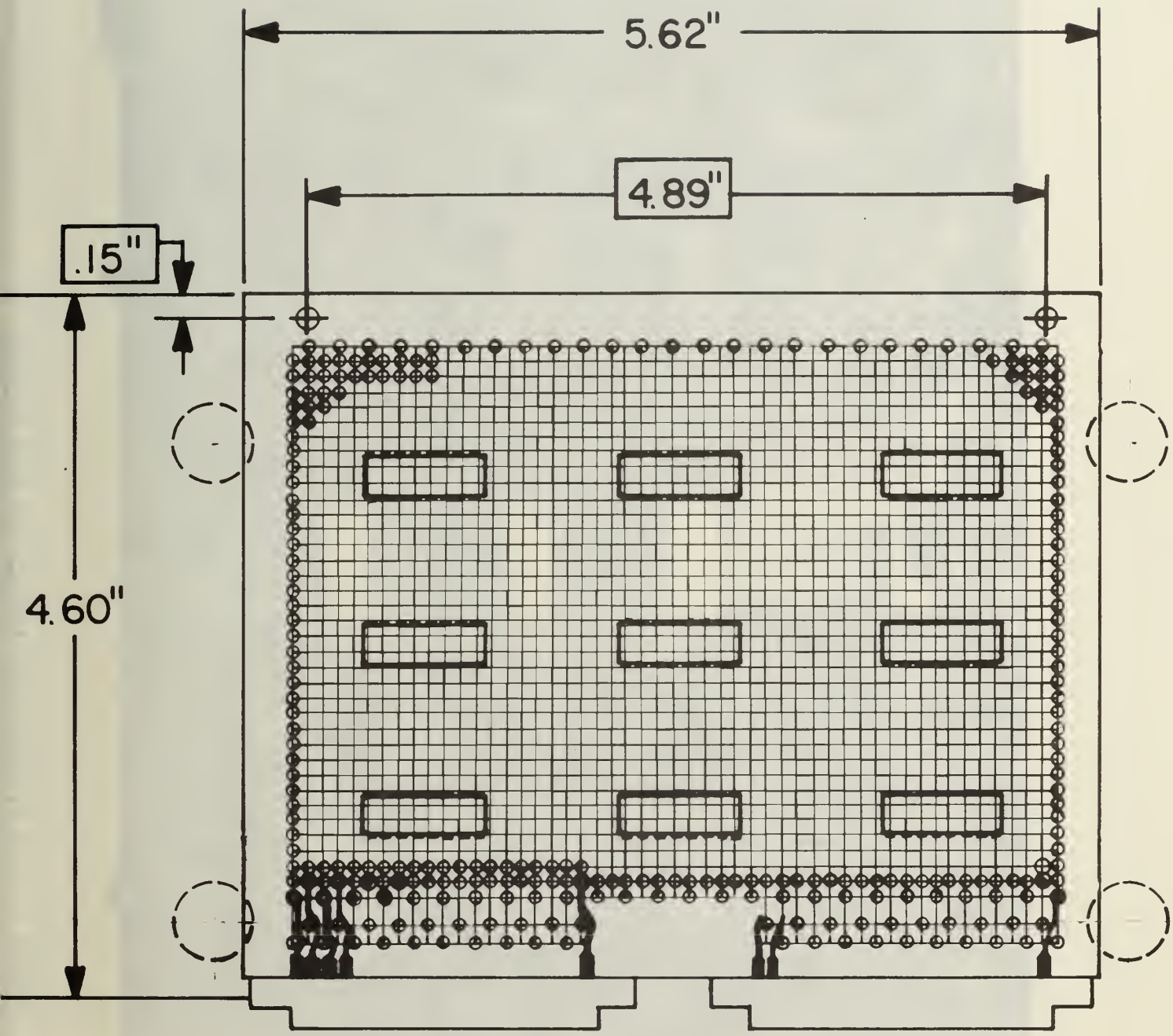

FIGURE 6 DETAILS OF CIRCUIT BOARD WITH RESISTORS

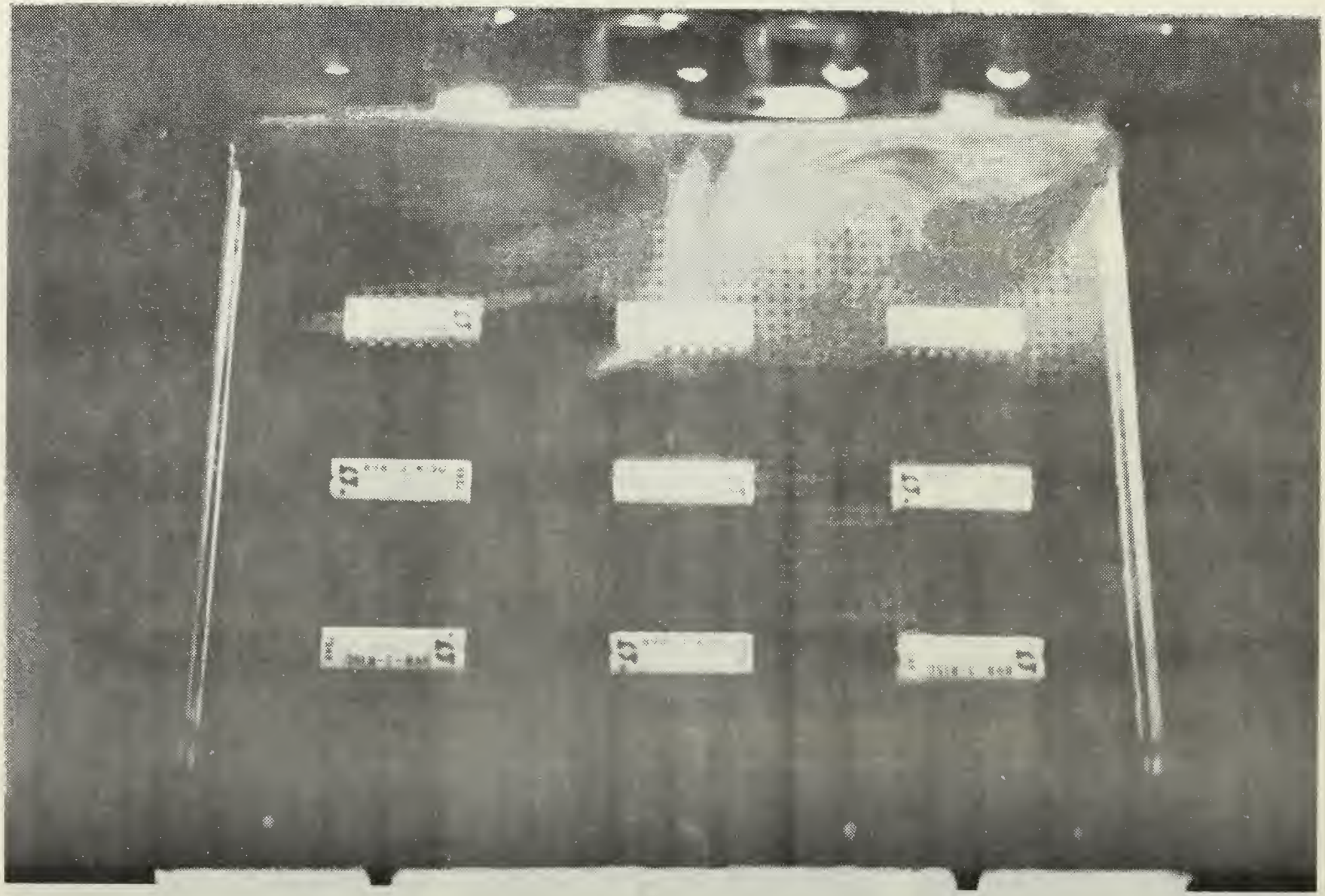

FIGURE 7 FLOW VISUALIZATION THROUGH THE TEST SECTION

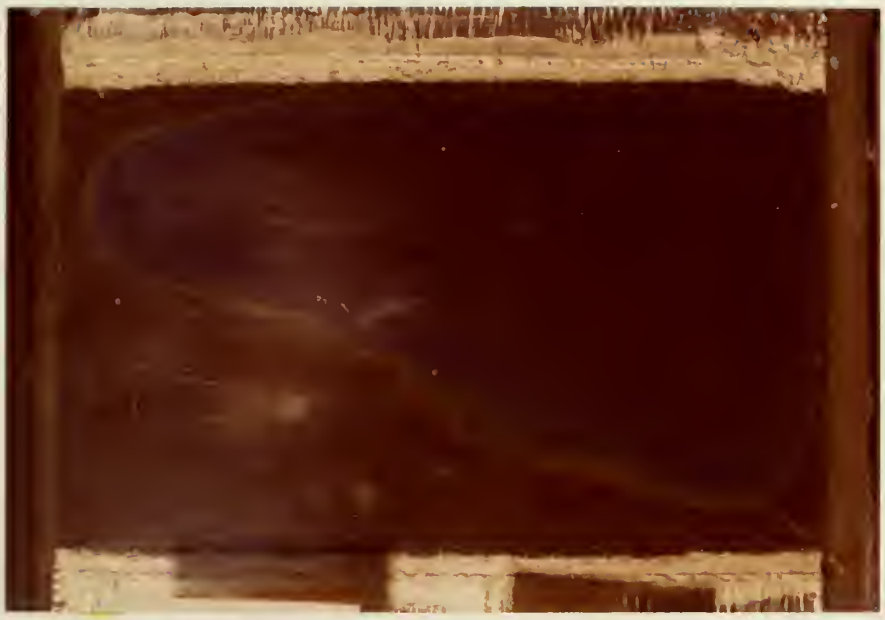

8(a)

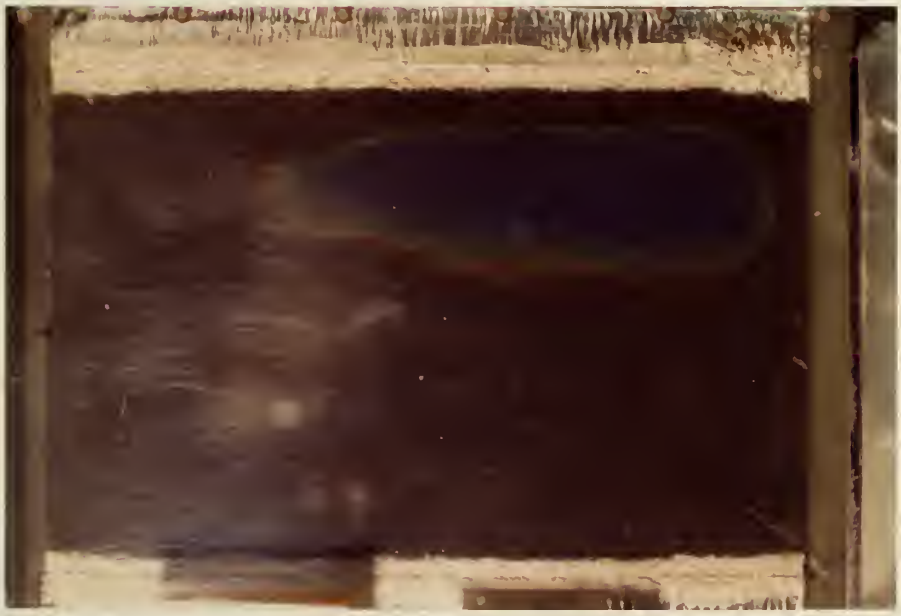

8(b)

FIGURE 8 VISUALIZATION OF TEMPERATURE VARIATIONS USING LIQUID CRYSTAL THERMOGRAPHY

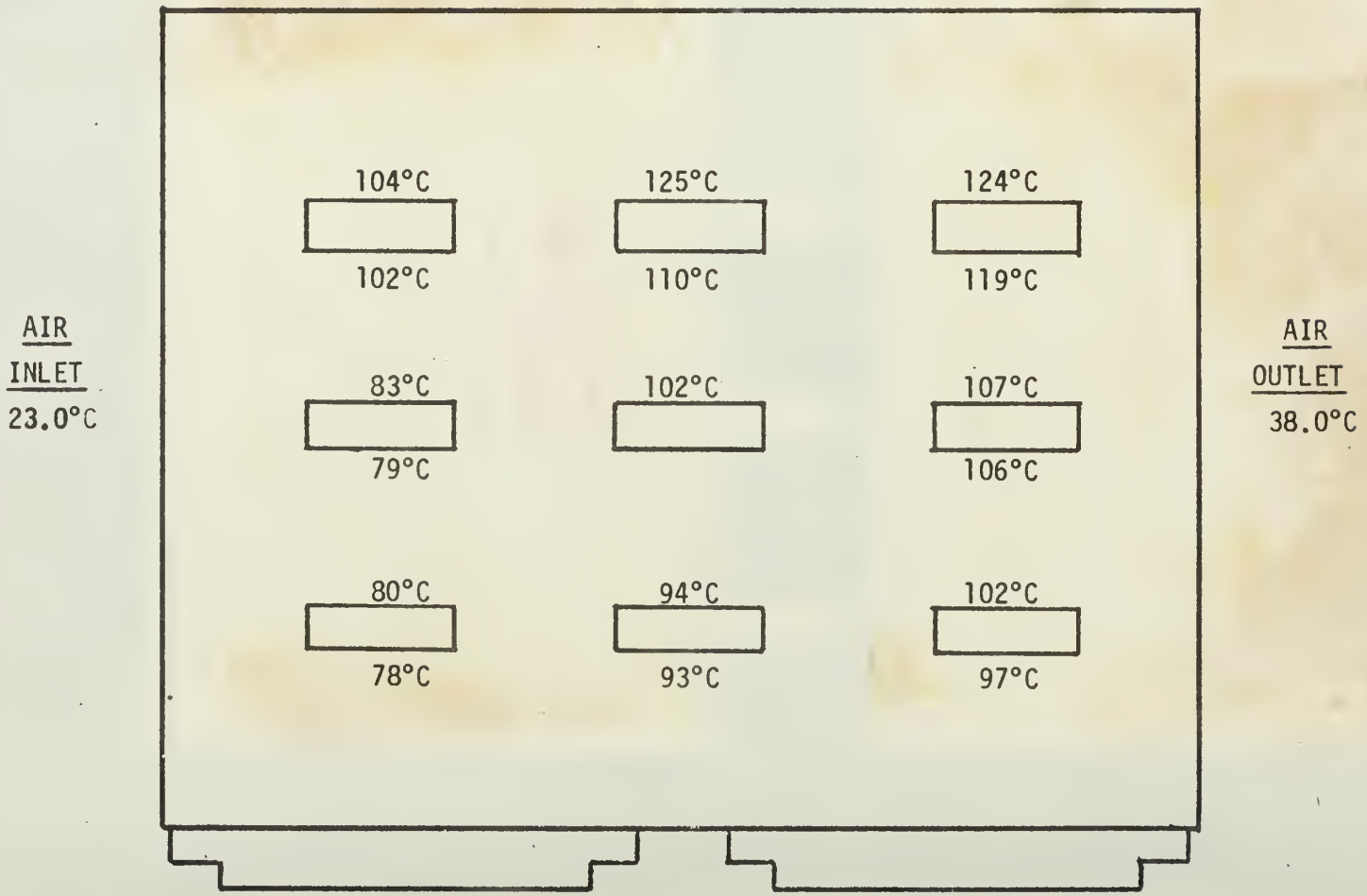

FIGURE 9 THERMOCOUPLE DATA FOR RUN 3, FIBERGLASS/EPOXY

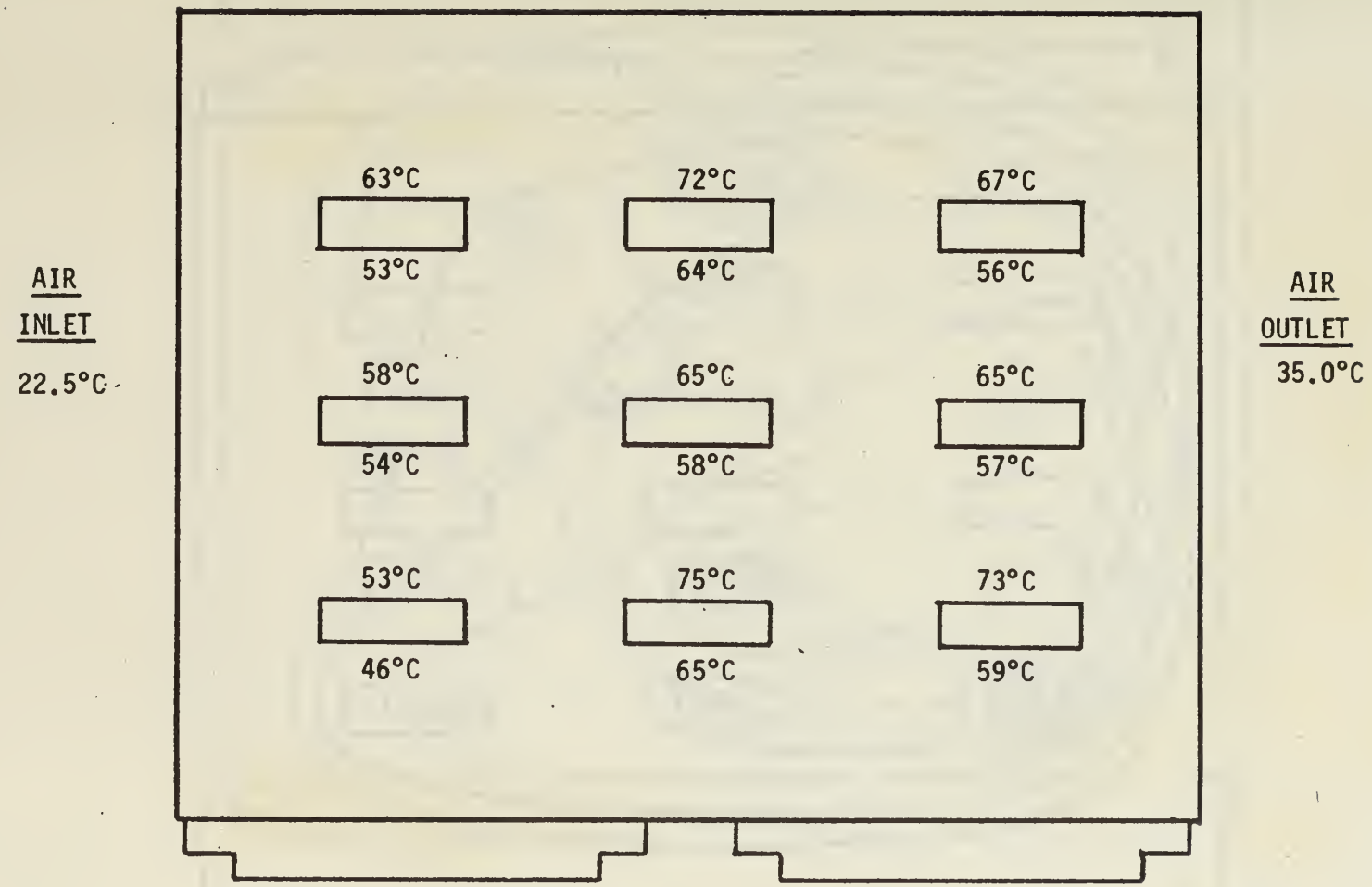

FIGURE 10 THERMOCOUPLE DATA FOR RUN 15, ALUMINUM CORE BOARD, 13.35 WATTS/BOARD, 0.73 CFM/BOARD

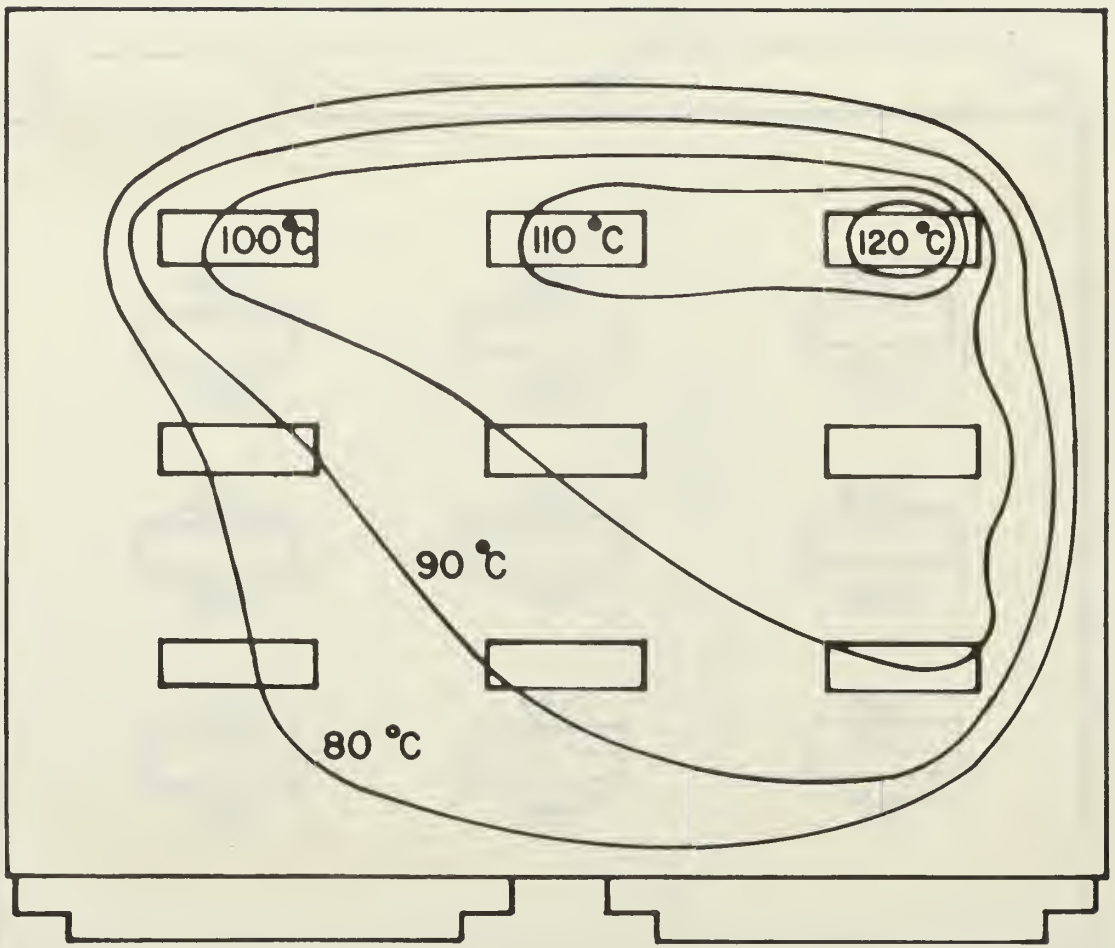

FIGURE 11 SCHEMATIC REPRESENTATION OF ISOTHERMS ON THE FIBERGLASS/EPOXY BOARD, 0.76 CFM/BOARD, 13.0 WATTS/BOARD

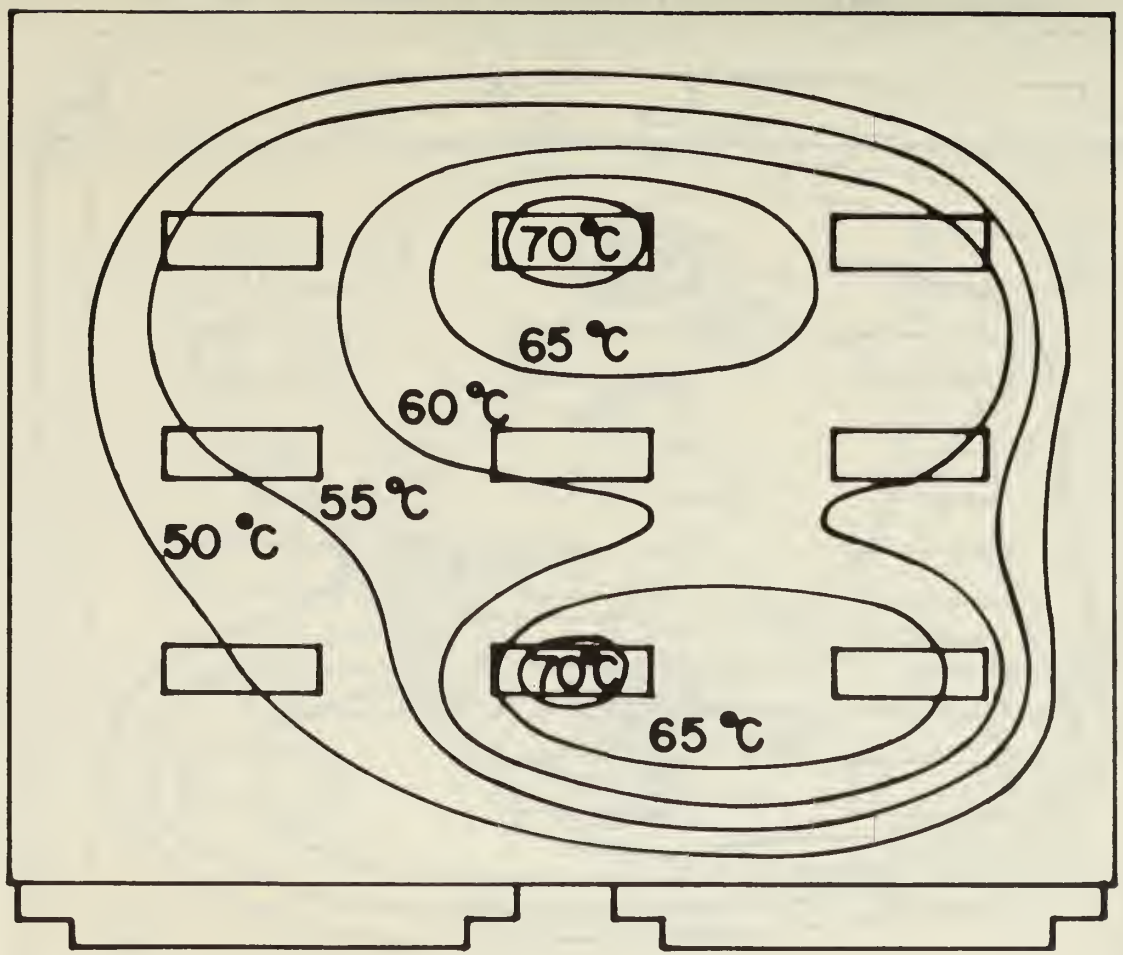

FIGURE 12 SCHEMATIC REPRESENTATION OF ISOTHERMS ON THE ALUMINUM CORE BOARD, 0.73 CFM/BOARD, 13.0 WATTS/BOARD

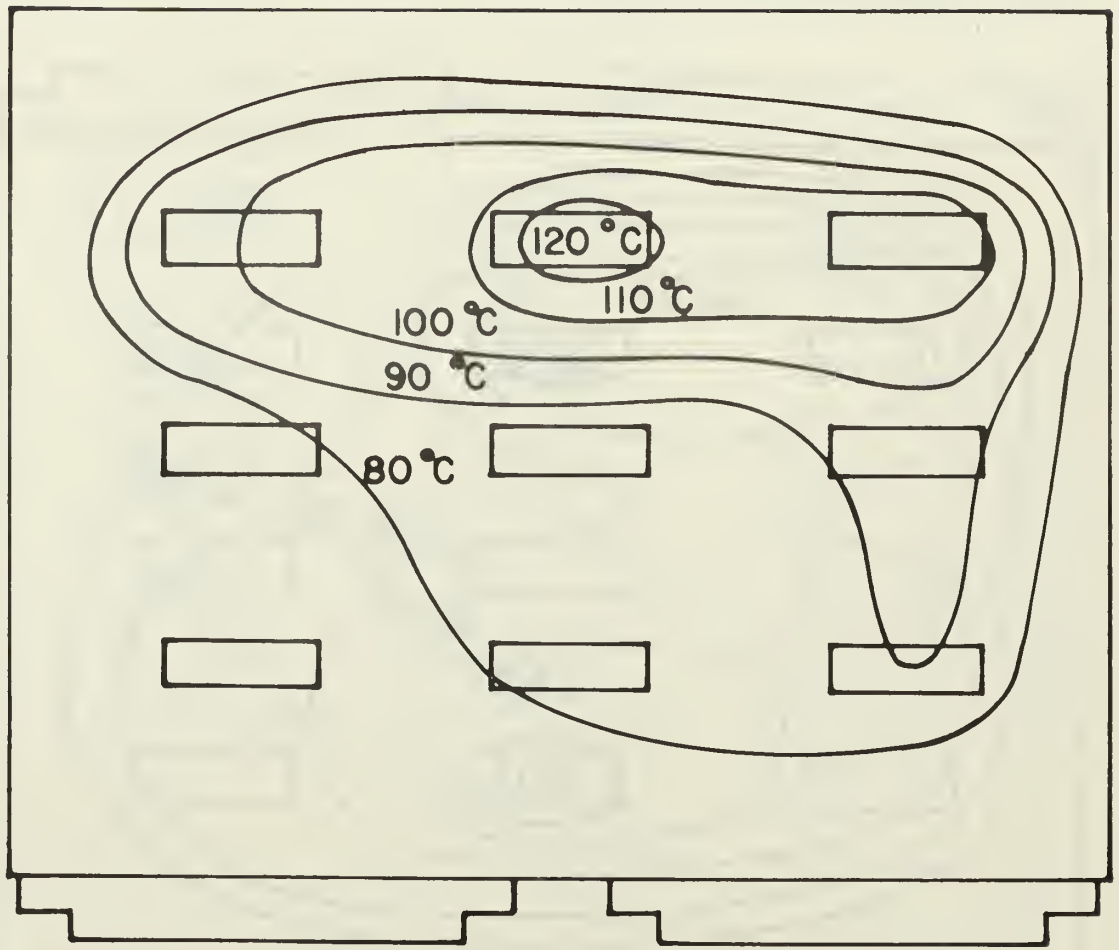

FIGURE 13 SCHEMATIC REPRESENTATION OF ISOTHERMS ON THE FIBERGLASS/EPOXY BOARD, 3.31 CFM/BOARD, 18.1 WATTS/BOARD

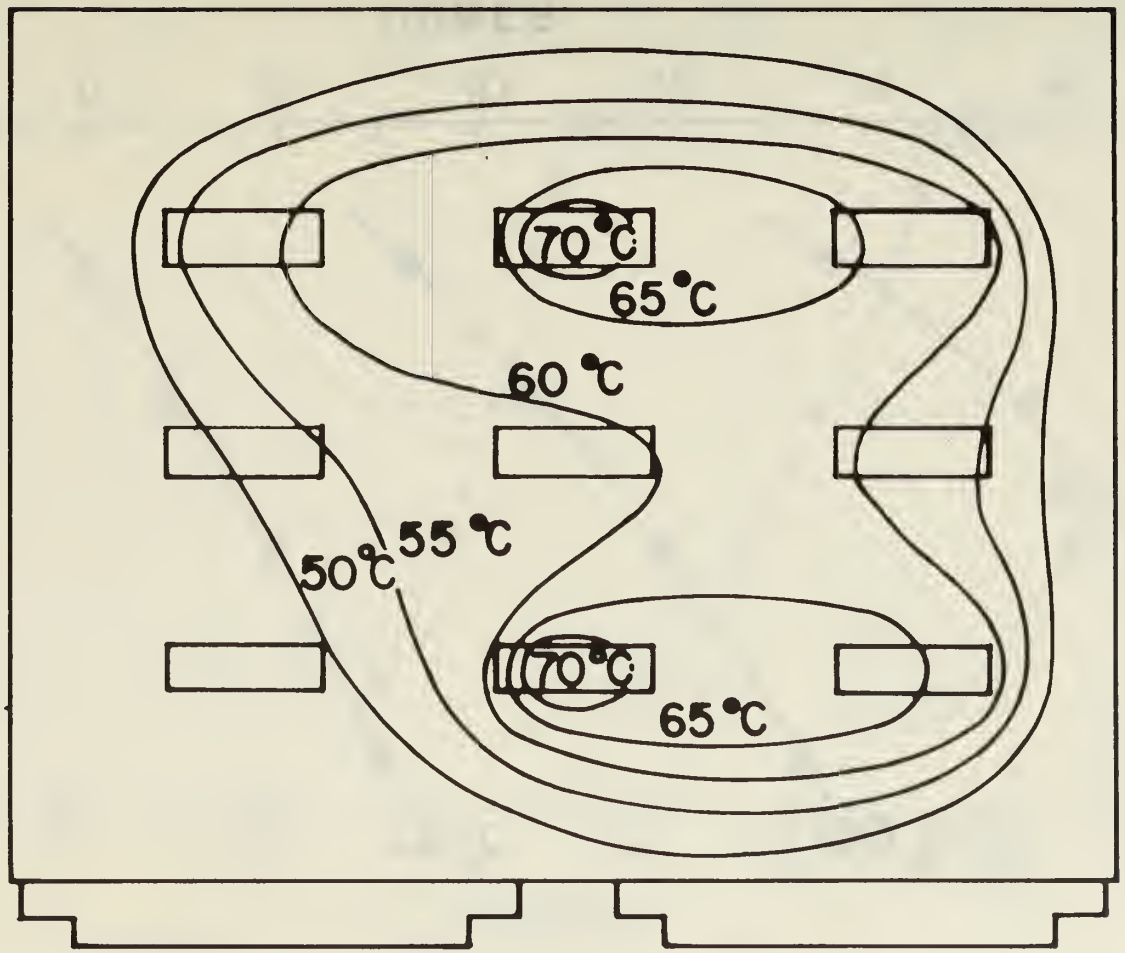

FIGURE 14 SCHEMATIC REPRESENTATION OF ISOTHERMS ON THE ALUMINUM CORE BOARD, 3.37 CFM/BOARD, 18.0 WATTS/BOARD

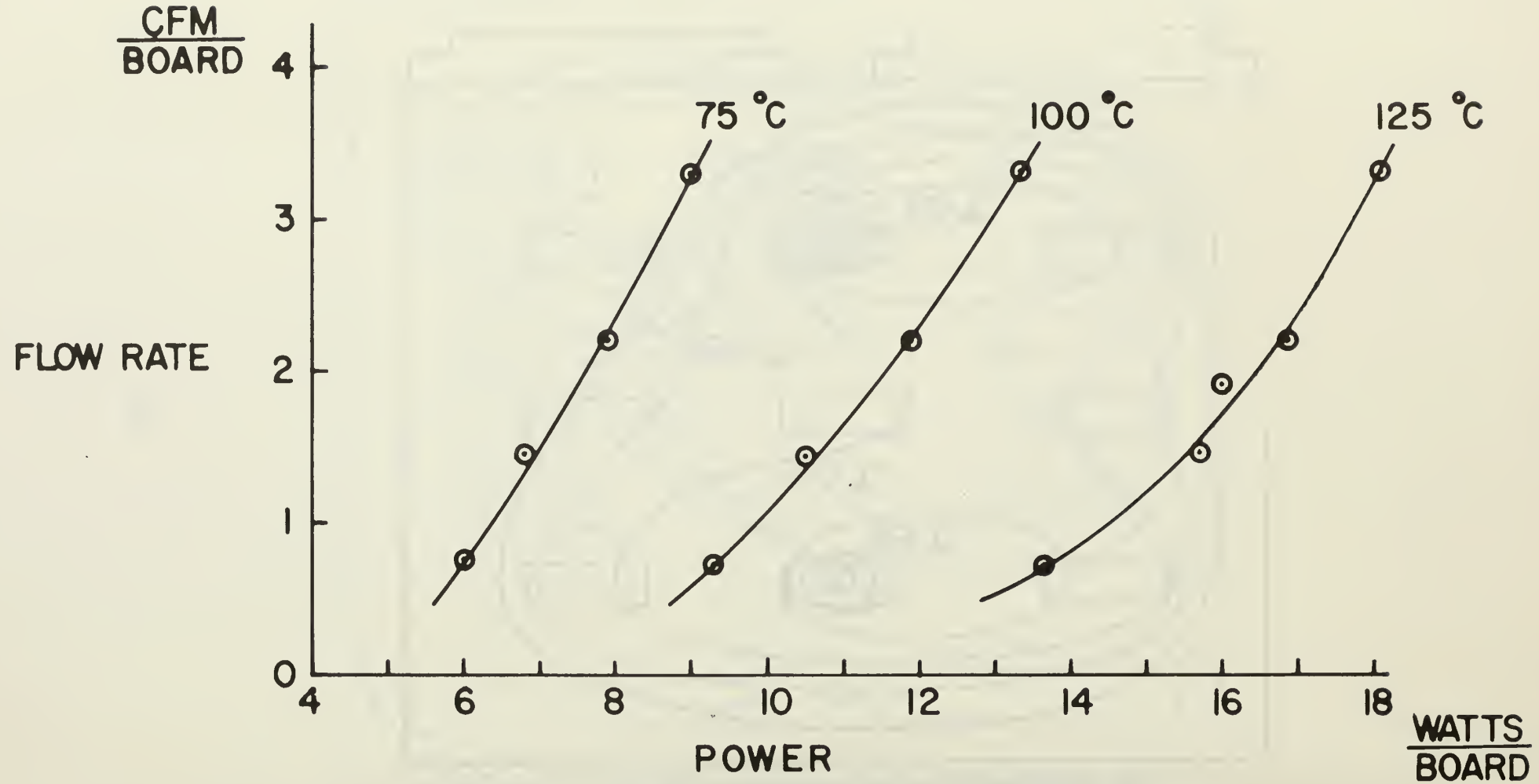

FIGURE 15 HOT SPOT THERMAL PERFORMANCE DATA FOR FIBERGLASS/EPOXY BOARD

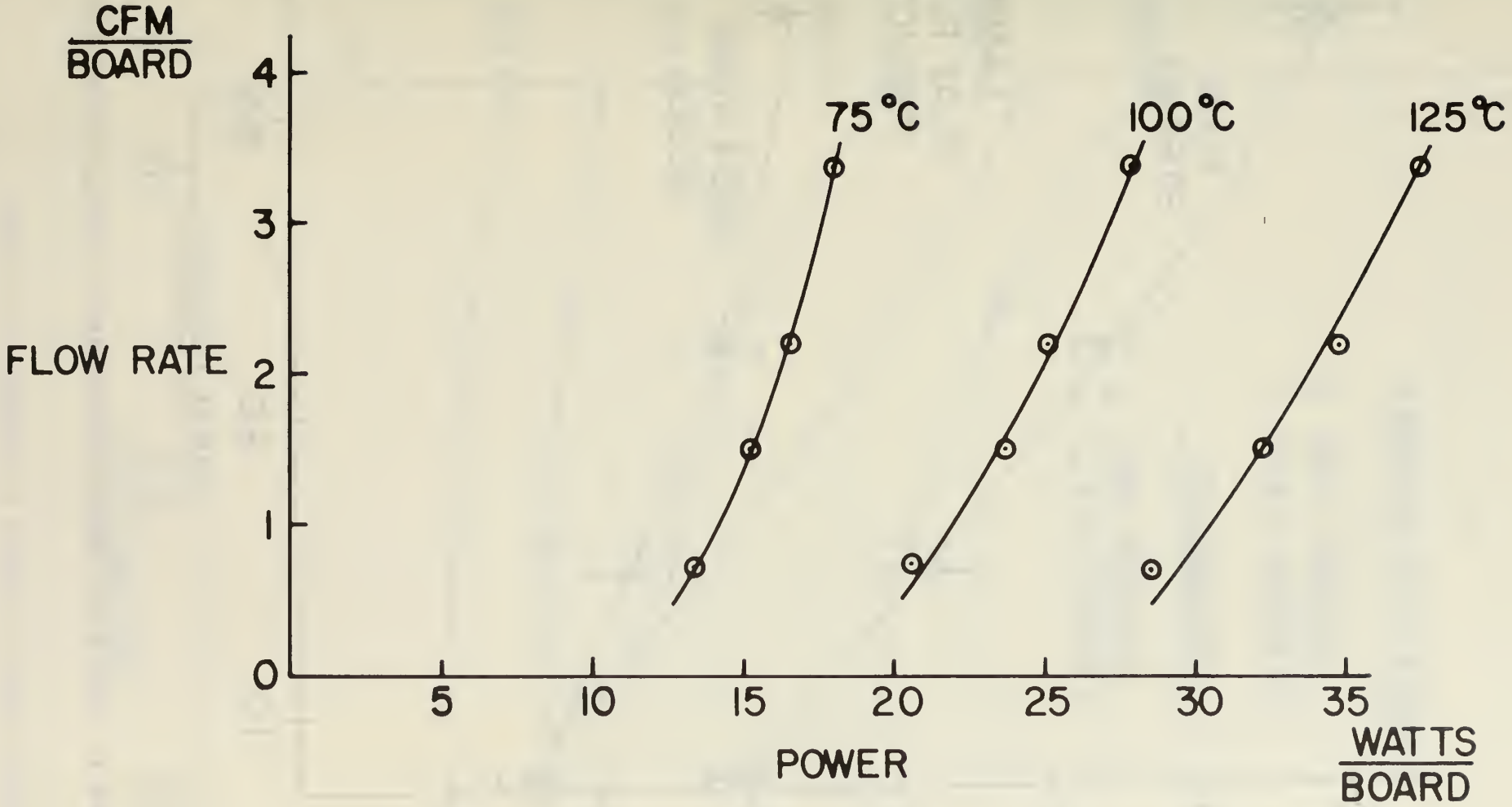

FIGURE 16 HOT SPOT THERMAL PERFORMANCE DATA FOR ALUMINUM CORE BOARD

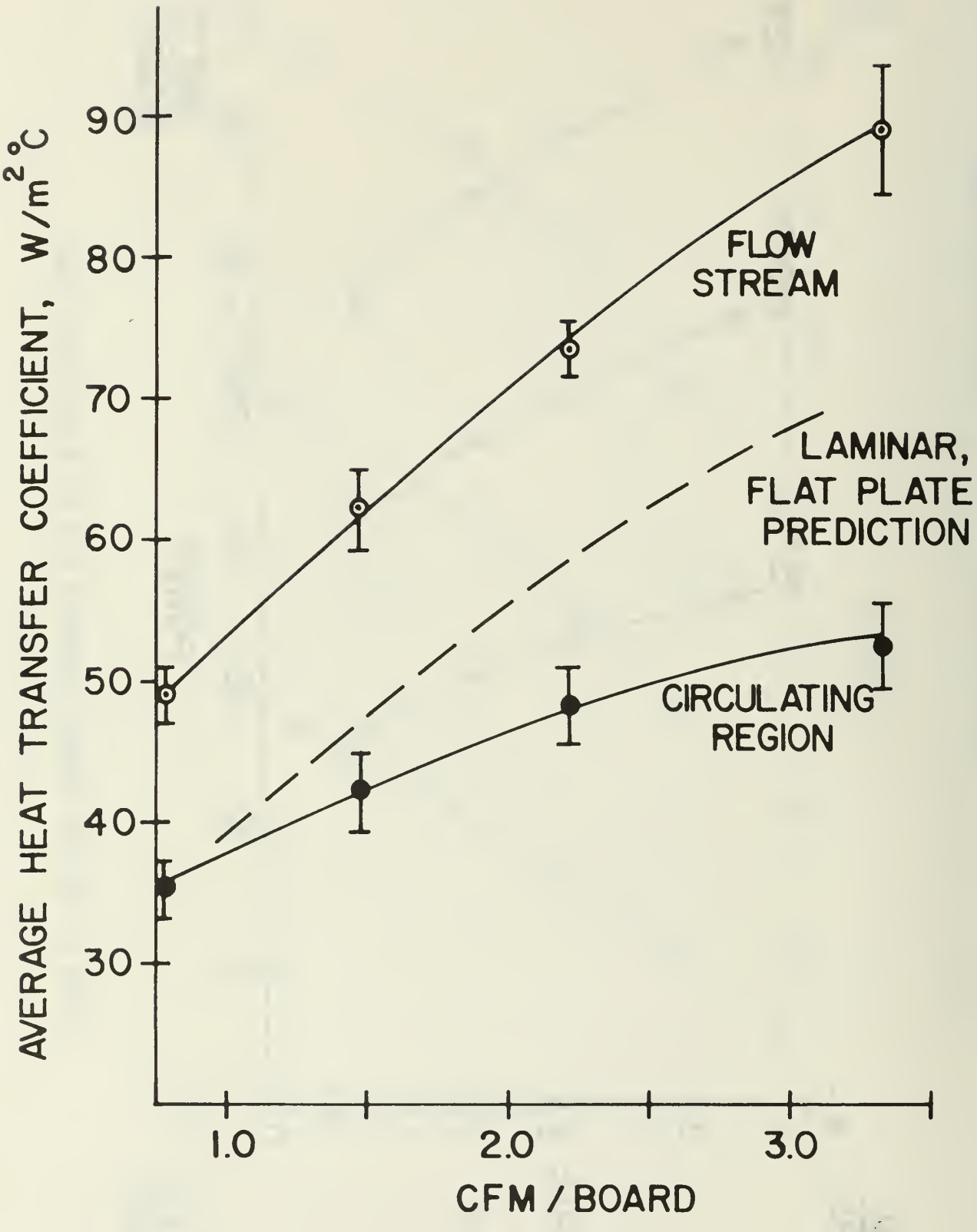

FIGURE 17 AVERAGE HEAT TRANSFER COEFFICIENT ON FIBERGLASS/EPOXY BOARD

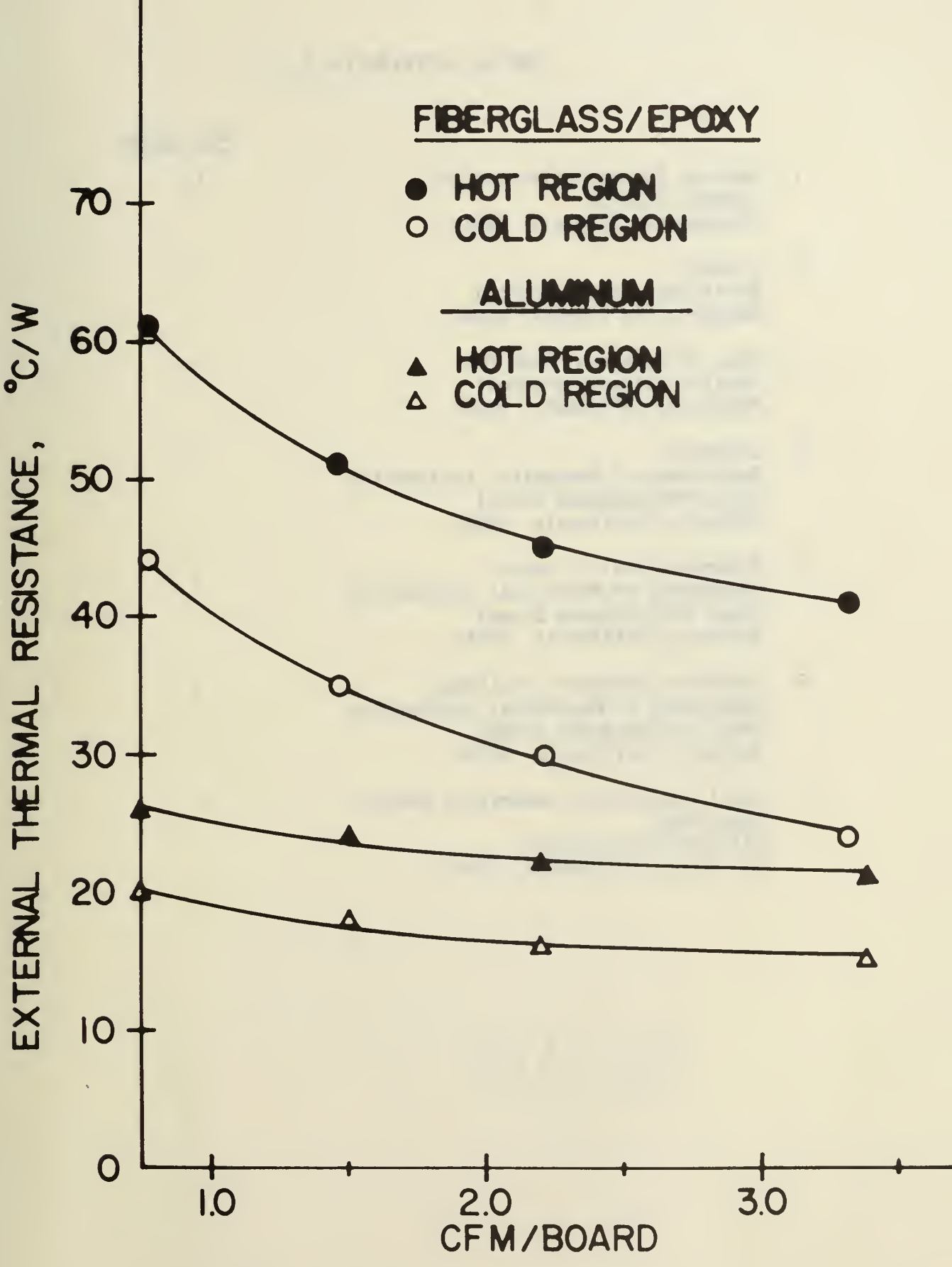

FIGURE 18 COMPARISON OF EXTERNAL THERMAL RESISTANCES

INITIAL DISTRIBUTION LIST

		No. Copies
1.	Defense Documentation Center Cameron Station Alexandria, Virginia 22314	12
2.	Library Naval Postgraduate School Monterey, California 93940	2
3.	Dean of Research, Code 023 Naval Postgraduate School Monterey, California 93940	1
4.	Chairman Department of Mechanical Engineering Naval Postgraduate School Monterey, California 93940	1
5.	Professor Paul J. Marto Department of Mechanical Engineering Naval Postgraduate School Monterey, California 93940	5
6.	Professor Matthew D. Kelleher Department of Mechanical Engineering Naval Postgraduate School Monterey, California 93940	5
7.	Naval Electronics Laboratory Center Code 4400 271 Catalina Boulevard San Diego, California 92152	10